Multipartite Entanglement Measure: Genuine to Absolutely Maximally Entangled

Rahul V1,* and S. Aravinda1,†

¹Indian Institute of Technology Tirupati, Tirupati, India 517619

Multipartite entanglement is a fundamental aspect of quantum mechanics, crucial to advancements in quantum information processing and quantum computation. Within this field, Genuinely Multipartite Entanglement (GME), being entangled in all bipartitions, and Absolutely Maximally Entanglement (AME), maximally entangled in all bipartitions, represent two significant types of entanglement with diverse applications. In this work, we introduce a new measure called the GME-AME multipartite entanglement measure, with a non-zero value representing the GME states and the maximum value is reached only by the AME states. The measure is applied to study the multipartite entanglement of four partite systems using the operator to state mapping, and the four partite permutation qutrit states are classified according to the measure. With various examples, we show that our measure is robust in classifying the four partite entangled states.

I. INTRODUCTION

Quantum entanglement is a quintessential property of a joint quantum system necessary for various information-theoretic advantages and quantum computation. Entanglement between two parties, referred to as bipartite entanglement, is theoretically well-studied and operationally quantified using various information-theoretic tasks. In these tasks, it can be cleraly shown the advantage of bipartite quantum entanglement [1, 2] over the any classical resources [3, 4]. Many questions in the bipartite mixed state entanglement persist; the bipartite pure state entanglement is well established. In many-body quantum theory, even though the system consists of many quantum particles, most of the existing study divides the entire many-body system into a bipartition and studies it as a high dimensional bipartite system [5]. The importance of entanglement and its structure enables important studies in quantum many-body systems, which in turn shape the fields of condensed matter theory and quantum gravity [6, 7].

The multipartite entanglement theory involves the entanglement shared among three or more subsystems. Unlike bipartite systems, multipartite systems exhibit a much richer and more intricate structure of entanglement, characterized by different forms and classifications. For any quantum computational advantage over classical computation, multipartite entanglement is necessary, but it's not sufficient. For example, in measurement-based quantum computation [8], only certain classes of multiparty entangled states are useful as resource states. For any clear understanding of the advantages of quantum computation and for the construction of successful algorithms, a deeper understanding of multiparty entanglement is essential.

The bipartite entanglement theory cannot be linearly lifted to multiparty level. There are various issues like defining the maximal entangled state [9], classification of multipartite entangled states under LOCC [10, 11], limitations of entanglement measures for multipartite systems [12], complexities in entanglement distillation and manipulation [13], and the challenges associated with extending Bell inequalities and nonlocality arguments to multipartite systems [14, 15].

Genuine multipartite entanglement (GME) and Absolutely Maximally entangled (AME) are the two main types of multipartite entanglement that we are interested in this work. Genuine multipartite entangled state that cannot be factored across any bipartition [16-18], whereas absolutely maximally entangled state exhibits maximum entanglement in all the possible bipartitions [19]. The construction of AME states has been explored through various mathematical approaches, such as combinatorial designs, stabilizer codes, and tensor networks [20-23]. The existence of AME states for a general number of systems and local dimensions still remains open, indicating ongoing challenges in characterizing these intriguing quantum states [24]. It has been proven that there are no AME states in the fourpartite qubit case [25].

Quantifying GME is crucial for understanding its properties and applications [26]. Various measures have been developed to characterize GME states. One widely-used approach is the geometric measure of entanglement, which has been the focus of extensive research efforts [27–33]. The analysis of density matrix elements also plays a significant role in examining the separability and classification of different GME states [34]. Numerous studies have employed concurrence-based [35, 36] methods to charecterise multipartite entanglement structures [26, 30, 37]. Several other entanglement measures have been developed to understand multipartite entanglement [38–41]. The Concentratable Entanglement generalizes various existing measures [42] in which its operational meaning is tied to the

^{*} rahulsomasundar@gmail.com

[†] aravinda@iittp.ac.in

probability of finding Bell pairs between qubits across different copies of the state.

GME states find applications in quantum sensing [43], quantum cryptography [44], and in quantum metrology [45]. In addition, they play a significant role in quantum networks, where their entangled nature allows for efficient entanglement distribution and resource sharing among multiple nodes [46]. AME states are equivalent to error correcting codes [47] and have application in secrete sharing [19], quantum repeters [48] and also in quantum gravity models [49]. Overall, multipartite states' versatile applications underscore their importance in the ongoing development of quantum technologies.

In this work, we construct a measure that can detect both GME and AME, and we term it the GME-AME multipartite entanglement measure. The non-zero value of the GME-AME measure implies the existence of GME states, and the maximum value is reached only by the AME states. As a specific application, we consider the four partite system and studied the GME-AME measure quantitatively. Using the operator state mapping, we construct a class of four party entangled states and calculate the GME-AME measure for this class. We compare the GME-AME with other independent GME measures and AME measures. By using the mapping between permutation operator to permutation states, the entanglement for four party qutrit is studied.

The paper is organized as follows: In Sec. (II), the multipartite entanglement is introduced and the GME-AME measure is constructed. A brief introduction to other measures is also provided. The operator to state mapping for a four-party system is developed, and its corresponding entanglement measure is calculated in Sec. (III. For four qubit systems, the GME-AME measure, along with other measures, are calculated in Sec. (IV) and for permutation states in Sec. (V). Finally concluded in Sec. (VI).

II. MULTIPARTITE ENTANGLEMENT MEASURES

Let \mathcal{H}_d denote the d dimensional Hilbert space of a single system, and the n partite Hilbert space is denoted as $\mathcal{H}_d^{\otimes n} \equiv \mathcal{H}_d \otimes \mathcal{H}_d \otimes \cdots \otimes \mathcal{H}_d$. The pure bipartite state $|\psi\rangle_{12}$ is called entangled if it cannot be written in product form as $|\psi\rangle_{12} = |\phi\rangle_1 \otimes |\phi\rangle_2$. The complexity of characterizing the nature of entanglement increases as the number of parties increases beyond two. There are distinct ways of defining, quantifying and characterizing multipartite entanglement. In this work, we are interested in two variants of multipartite entangled states, genuinely multipartite entangled (GME) and absolutely maximally entangled (AME) pure states.

An *n* partite state is fully separable if it can be written as a pure product state $|\Psi\rangle = |\psi_1\rangle_1 \otimes \cdots |\psi_n\rangle_n$, otherwise it is entangled. If the state $|\Psi\rangle$ is entangled but remains in product form $|\Psi\rangle = |\phi\rangle_A \otimes |\varphi\rangle_{A^c}$ in any bipartition A/A^c , then $|\Psi\rangle$ is called biseparable. The state $|\Psi\rangle$ is called a GME if it is not biseparable, it is entangled in all bipartitions. The state $|\Psi\rangle$ is AME if the reduced state ρ_A of any bipartition A/A^c is a maximally mixed state i.,e $\rho_A \propto I \quad \forall A$. All AME are GME but the converse is not true. The relaxed version of AME is the k -uniform states, which is defined as all the reduced states of *k* partites are proportional to the idenity. The AME corresponds to $k = \lfloor n/2 \rfloor$. A non-AME k uniform state could be non-GME. A simple example to demonstrate the differences is that a three-partite GHZ state is AME and also GME, while the three-partite W state is GME but not AME, and a *n*-partite GHZ state is GME but not AME, but is 1-uniform.

As we have explained in the Introduction, there are many measures and witness for a GME and various constructions for AME states. Here we are interested to construct a measure that will witness the GME and also the AME, and we call it the *GME-AME* measure. The GME-AME measure $\mathbb{E}(|\Psi\rangle)$ should satisfy the following conditions:

- 1. $\mathbb{E}(|\Psi\rangle) = 0$ for all biseparable states. This implies that if $\mathbb{E}(|\Psi\rangle) > 0$, the state $|\Psi\rangle$ is GME.
- 2. $\mathbb{E}(|\Psi\rangle) = 1$ if and only if the state $|\Psi\rangle$ is AME.

We propose the following measure that satisfies the above conditions:

$$\mathbb{E}(|\Psi\rangle) = \left(\frac{d}{d-1}\right)^{m_1} \left(\frac{d^2}{d^2-1}\right)^{m_2} \cdots \left(\frac{d^{\frac{n}{2}}}{d^{\frac{n}{2}}-1}\right)^{m_k} \prod_{i_1=1}^{m_1} \left(1 - \operatorname{Tr} \rho_{i_1}^2\right) \prod_{i_2=1}^{m_2} \left(1 - \operatorname{Tr} \rho_{i_2}^2\right) \cdots \prod_{i_k=1}^{m_k} \left(1 - \operatorname{Tr} \rho_{i_k}^2\right). \tag{1}$$

Here m_l is the total number of all possible bipartitions

of the reduced state of l partite and ρ_{i_l} is a reduced den-

sity matrix of l partite with $l \in \{1, 2, \dots \lfloor \frac{n}{2} \rfloor \}$. Here m_l is the total number of all possible bipartitions of l partite reduced state and ρ_{i_l} is an l-partite reduced density matrix with $l \in \{1, 2, \dots \frac{n}{2} \}$.

The reduced state ρ_{i_l} will be the pure state if the corresponding bipartition is separable, resulting in a biseparable state $|\Psi\rangle$ hence $\mathbb{E}(|\Psi\rangle)=0$, and implies that for any $\mathbb{E}(|\Psi\rangle)>0$ state is GME. $\mathbb{E}(|\Psi\rangle)=1$ if and only if $|\Psi\rangle$ is an AME follows from the fact that if the state $|\Psi\rangle$ is AME, the reduced density matrix of all the bipartitions will be maximally mixed and hence the measure $\mathbb{E}(|\Psi\rangle)$ reaches the maximum values 1 (the constants are normalized accordingly), conversely the purity $1-\mathrm{tr}(\rho_i^2)$ is maximum only for the corresponding maximally mixed state $\rho_i \propto I$.

The two unitary operators U and U' are said to be LU invariant if $U' = (u_1 \otimes u_2 \otimes \cdots \otimes u_n)U(u'_1 \otimes u'_2 \otimes \cdots \otimes u'_n)$. The GME-AME measure $\mathbb{E}(|\Psi\rangle)$ is invariant under the local unitary transformation. For any bipartition, the spectrum of the reduced state is LU invariant and hence the measure $\mathbb{E}(|\Psi\rangle)$ is also LU invariant, and it is non-increasing on average under LOCC [42].

In this work we are mainly interested in two other related measures for comparision. The first one is due to Scott [50], which we call here as the Scott measure [50] and is defined as follows:

$$\operatorname{Sct}_k(|\psi\rangle) := \frac{d^k}{d^k - 1} \left(1 - \frac{k!(n-k)!}{n!} \sum_{|S| = k} \operatorname{Tr} \rho_s^2 \right) \tag{2}$$

where $k = 1, 2, \dots, \lfloor n/2 \rfloor, \lfloor \rfloor$ denotes the lowest integer part and $S \subset \{1, 2, \dots, n\}$.

Some of the properties of Sct_k

- 1. $0 \leq \mathbb{S}ct_k \leq 1 \quad \forall k$
- 2. $Sct(|\psi\rangle) = 0$ if and only if $|\psi\rangle$ is a pure product state, i.e., $|\psi\rangle = \bigotimes_{j=1}^{n} |\psi_j\rangle$.
- 3. $Sct_k(|\psi\rangle) = 1$ if and only if $|\psi\rangle$ is *k*-uniform, that is all *k* partite reduced state are maximally mixed.

Similarly, the GME measure that we are interested in in this work is based on the triangle measure by Xie et al. [31], and extended to the four qubits system in Ref. [32]. This measure uses geometric intuition to quantify the genuine entanglement. The GME measure for four-qubit system is defined using the volume *V* of a simplex polygon, which is given as:

$$V = \frac{\sqrt{2}}{3} S^{1/2} (R_0 R_1 R_2 R_3)^{1/4}, \tag{3}$$

where the coefficients R_0 , R_1 , R_2 , R_3 and S are functions of the pairwise correlations γ_{ij} , and γ_{ij} are the area of

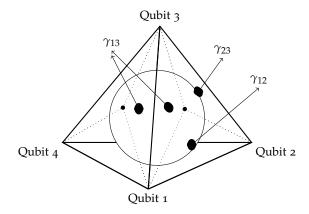


Figure 1. Tetrahedron with qubits on its 4 vertices, each face is divided into 3 triangle and its area is denoted as γ_{12} , γ_{13} , γ_{23} and γ_{ij} is the area of triangle by the qubit i, qubit j and the mid point of that face

the polygon shown in Fig. (1) are:

$$R_{0} = +\sqrt{\gamma_{12}\gamma_{34}} + \sqrt{\gamma_{13}\gamma_{24}} + \sqrt{\gamma_{14}\gamma_{23}}$$

$$R_{1} = -\sqrt{\gamma_{12}\gamma_{34}} + \sqrt{\gamma_{13}\gamma_{24}} + \sqrt{\gamma_{14}\gamma_{23}}$$

$$R_{2} = +\sqrt{\gamma_{12}\gamma_{34}} - \sqrt{\gamma_{13}\gamma_{24}} + \sqrt{\gamma_{14}\gamma_{23}}$$

$$R_{3} = +\sqrt{\gamma_{12}\gamma_{34}} + \sqrt{\gamma_{13}\gamma_{24}} - \sqrt{\gamma_{14}\gamma_{23}}$$

$$S = 2(\gamma_{12} + \gamma_{13} + \gamma_{14} + \gamma_{23} + \gamma_{24} + \gamma_{34})$$
(4)

The $\gamma's$ can be obtained by simultaneously solving the following Eq. (5).

$$\gamma_{ij} + \gamma_{ik} + \gamma_{il} = E_{i|jkl}
-\sqrt{\gamma_{ij}\gamma_{kl}} + \sqrt{\gamma_{ik}\gamma_{jl}} + \sqrt{\gamma_{il}\gamma_{jk}} = \lambda E_{ij|kl},$$
(5)

where $E_{ij|kl}$ and $E_{i|jkl}$ are bipartite and single partite von Neumann entropies. The polygon measure \mathbb{P} is defined as

$$\mathbb{P} = \frac{3^{7/6}}{2} V^{2/3}.\tag{6}$$

Here $0<\mathbb{P}\leq 1$ for all GME states and $\mathbb{P}=0$ for any non-GME states.

III. ENTANGLEMENT OF FOUR PARTITE SYSTEM

Many interesting properties of the four partite systems can be studied by using operator to state mapping, the Choi-Jamialkowski isomorphism, as the operator acting on two systems can be mapped to four partite systems. A $d \times d$ matrix (an operator) $A = \sum_{ij} \langle i|A|j\rangle |i\rangle\langle j| \in \mathcal{H}_d$ can be mapped to a state $|A\rangle_{12} = \frac{1}{\sqrt{d}} \sum_{ij} \langle i|A|j\rangle |ij\rangle \in \mathcal{H}_d \otimes \mathcal{H}_d$. Similarly, an operator $A = \sum_{i\alpha,j\beta} \langle i\alpha|A|j\beta\rangle |i\alpha\rangle\langle j\beta| \in \mathcal{H}_d \otimes \mathcal{H}_d$ is mapped to a

four partite state $|A\rangle_{1234}=\frac{1}{d}\sum_{i\alpha,j\beta}\langle i\alpha|A|j\beta\rangle\,|i\alpha j\beta\rangle\,$ [51]. By using the vectorization identity $|XYZ\rangle=(Z^T\otimes X)\,|Y\rangle$, the local unitarily (LU) invariant operators $A'=u_1\otimes u_2Au_3\otimes u_4$ is mapped to LU invariant four party state as $|A'\rangle=u_3^T\otimes u_4^T\otimes u_1\otimes u_2\,|A\rangle$, thereby preserving all the entanglement structures. Here T represents full transpose, $\langle i\alpha|A|j\beta\rangle=\langle j\beta|A^T|i\alpha\rangle$.

The two-particle reduced density matrix takes a simple form in this representation, easing many calculations. For that, we need to define various reshaping maps of the matrix [51, 52]. The realignment and partial transpose are such reshaping operations that are widely used in the entanglement theory [53, 54] and open quantum systems [55, 56]. Recently, these operations are involved in defining the solvable models of many-body systems and have provided a host of analytically solvable properties [57–61]. We use the following reshaping of matrices in our work:

Realignment 1:
$$\langle i\alpha|A|j\beta\rangle = \langle \beta\alpha|A^{R_1}|ji\rangle$$

Realignment 2: $\langle i\alpha|A|j\beta\rangle = \langle ij|A^{R_2}|\alpha\beta\rangle$
Partial Transpose 1: $\langle i\alpha|A|j\beta\rangle = \langle j\alpha|A^{T_1}|i\beta\rangle$ (7)
Partial Transpose 2: $\langle i\alpha|A|j\beta\rangle = \langle i\beta|A^{T_2}|j\alpha\rangle$.

In this terminology, for a four partite state

$$|A\rangle_{1234} = \frac{1}{d} \sum_{i\alpha,j\beta} \langle i\alpha | A | j\beta \rangle | i\alpha j\beta \rangle,$$
 (8)

the two particle-reduced density matrix is given as

$$\rho_{12} = \frac{AA^{\dagger}}{d^2}, \quad \rho_{13} = \frac{A^{R_2}A^{R_2\dagger}}{d^2}, \quad \rho_{14} = \frac{A^{T_2}A^{T_2\dagger}}{d^2}. \quad (9)$$

The advantage of this representation is visible by considering the measure $\mathbb{E}|\Psi\rangle$ for four parties,

$$\mathbb{E}(|\Psi\rangle) = \left(\frac{d}{d-1}\right)^4 \left(\frac{d^2}{d^2-1}\right)^3$$

$$\prod_{j=1}^4 (1 - \operatorname{tr} \rho_j^2) \prod_{r \in \{12,13,14\}} (1 - \operatorname{tr} \rho_r^2).$$
(10)

Suppose the two-particle operator A is unitary, $\rho_{12}=\frac{I}{d^2}$, and hence all single particle reduced state $\rho_j=\frac{I}{d}$ $\forall j\in\{1,\cdot,4\}$, and then the measure $\mathbb{E}(|\Psi\rangle)$ reduces to

$$\mathbb{E}(|\Psi\rangle) = \left(\frac{d^2}{d^2 - 1}\right)^2 (1 - \operatorname{tr} \rho_{13}^2) (1 - \operatorname{tr} \rho_{14}^2). \tag{11}$$

For the identity matrix $I = \sum ij |ij\rangle\langle ij|$, the realignment is $I^{R_2} = \sum_{ij} |ii\rangle\langle jj|$, hence the state $\rho_{13} = |\phi^+\rangle\langle\phi^+|$, where $|\phi^+\rangle = \frac{1}{\sqrt{d}}\sum_i |ii\rangle$, a two particle maximally entangled state [6o]. Hence, the state $|I\rangle$ and any LU

equivalent to $|I\rangle$ is non-GME for that $\mathbb{E}(|I\rangle) = 0$. Similarly, consider swap $S = \sum_{ij} |ji\rangle\langle ij|$, for which $S^{T_2} =$ $\sum_{ij} |jj\rangle\langle ii|$, hence the state $\rho_{14} = |\phi^+\rangle\langle\phi^+|$, that the state $|S\rangle$ and its LU equivalent is non-GME, and $\mathbb{E}(|I\rangle) = 0$. This provides an elegant way to construct any four partite GME states. Any diagonal unitary operator $U = \sum_{ij} e^{\theta_{ij}} |ij\rangle\langle ij|$ remains unitary after partial transposition T_2 , and the state $\rho_{14} = \frac{1}{d^2}$ 9, and hence except the identity operator *I* and its LU equivalent, $\mathbb{E}(|\Psi\rangle) > 0$. Similarly, except for SWAP and its LU equivalent, any unitary operator after realignment R_2 remains unitary, and its corresponding $|\Psi\rangle$ is GME. Such unitary operators are called dual-unitary operators [57, 58] and have been studied widely in many-body exactly solvable models. Various construction methods of such dual-unitary operators provide a host of four partite GME states.

IV. FOUR QUBIT STATES

The unitary operator U acting on two qubits is LU equivalent to a three-parameter family of unitary operators X expressed in its canonical called Cartan decomposition as [62-64]

$$X = \exp\left[-i(x\sigma_{x} \otimes \sigma_{x} + y\sigma_{y} \otimes \sigma_{y} + z\sigma_{z} \otimes \sigma_{z})\right]$$

$$= \begin{bmatrix} e^{-iz}c_{-} & 0 & 0 & -ie^{-iz}s_{-} \\ 0 & e^{iz}c_{+} & -ie^{iz}s_{+} & 0 \\ 0 & -ie^{iz}s_{+} & e^{iz}c_{+} & 0 \\ -ie^{-iz}s_{-} & 0 & 0 & e^{-iz}c_{-} \end{bmatrix}$$
(12)

where $c_{\pm} = \cos(x \pm y)$, $s_{\pm} = \sin(x \pm y)$ and $0 \le |z| \le y \le x \le \pi/4$. Thus the coefficients form a tetrahedron called a Weyl chamber represented in Fig. (2)

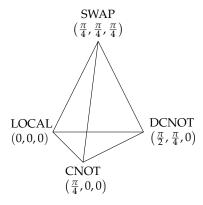


Figure 2. Weyl Chamber representation of LU equivalent parameterized nonlocal unitary operators, vertices are represented as LOCAL, CNOT, DCNOT, and SWAP gates with their corresponding parameter values.

The operator state mapping of the unitary operator X to $|X\rangle$ provides a parameterized set of four party

qubit states having various entanglement structure. The

GME-AME measure $\mathbb{E}(|X\rangle)$ can be calculated explicitly for the family of $|X\rangle$ states and given as :

$$\mathbb{E}(|X\rangle) = \frac{16}{9} \left(1 - \frac{1}{8} \left[\left(\cos^2(x - y) + \cos^2(x + y) \right)^2 + \left(\sin^2(x + y) + \sin^2(x - y) \right)^2 + (2\cos(x - y)\cos(x + y)\cos(2z))^2 \right] + (2\sin(x + y)\sin(x - y)\cos(2z))^2 \right]$$

$$+ (2\sin(x + y)\sin(x - y)\cos(2z))^2 \right]$$

$$+ \left(2\cos(x - y) + \sin^2(x + y) \right)^2 + \left(\cos^2(x + y) + \sin^2(x - y) \right)^2$$

$$+ (2\cos(x - y)\sin(x + y)\sin(2z))^2 + (2\cos(x + y)\sin(x - y)\sin(2z))^2 \right]$$

$$+ (3\cos(x - y)\sin(x + y)\sin(2z))^2 + (3\cos(x + y)\sin(x - y)\sin(2z))^2$$

$$+ (3\cos(x - y)\sin(x + y)\sin(2z))^2 + (3\cos(x + y)\sin(x - y)\sin(2z))^2 \right]$$

$$+ (3\cos(x - y)\sin(x + y)\sin(2z))^2 + (3\cos(x + y)\sin(x - y)\sin(2z))^2 \right]$$

$$+ (3\cos(x - y)\sin(x + y)\sin(2z))^2 + (3\cos(x + y)\sin(x - y)\sin(2z))^2$$

$$+ (3\cos(x - y)\sin(x + y)\sin(2z))^2 + (3\cos(x + y)\sin(x - y)\sin(2z))^2 \right]$$

$$+ (3\cos(x - y)\sin(x + y)\sin(2z))^2 + (3\cos(x + y)\sin(x - y)\sin(2z))^2$$

$$+ (3\cos(x - y)\sin(x + y)\sin(2z))^2 + (3\cos(x + y)\sin(x - y)\sin(2z))^2$$

$$+ (3\cos(x - y)\sin(x + y)\sin(2z))^2 + (3\cos(x + y)\sin(x - y)\sin(2z))^2$$

$$+ (3\cos(x - y)\sin(x + y)\sin(2z))^2 + (3\cos(x + y)\sin(x - y)\sin(2z))^2$$

The GME-AME measure is interesting to consider on the state $|X\rangle$ for the values corresponding to the edges of the Weyl chamber. For four qubit states, GME-AME can never take the maximum value of 1, as four qubit AME doesn't exist [25]. The GME-AME values for the state $|X\rangle$ has been plotted for various values of [x,y,z] in Fig. (3). For the single parameter family, the plot ranges for all the values, and for two and three parameter family, we have considered the equal values for all the parameters to satisfy the Weyl condition.

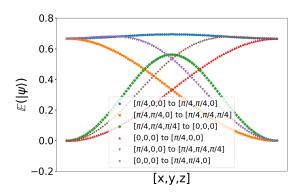


Figure 3. The value of GME-AME measure $\mathbb{E}(|X\rangle)$ varying the Weyl parameters [x,y,z]. It is generated from 100 data points obtained by varying the values of [x,y,z] satisfying Weyl condition.

For the line connecting between LOCAL and SWAP for values (0,0,0) to $(\frac{\pi}{4},0,0)$, X^{T_2} is unitary and hence the reduced state ρ_{14} 9 is maximally mixed, and the corresponding GME-AME value is

$$\mathbb{E}(|X\rangle) = \frac{1 - \cos(4x)}{3},\tag{14}$$

for which the maximum value 2/3 is reached for the value $x=\pi/4$ and the 0 for the value x=0. Similarly, for the edge between SWAP to DCNOT, $(\frac{\pi}{4},\frac{\pi}{4},\frac{\pi}{4})$ to $(\frac{\pi}{4},\frac{\pi}{4},0)$, the reduced matrix ρ_{13} is maximally mixed and the GME-AME value varies between 0 and 2/3 for z=0 to $z=\pi/4$, and for other value the expression is given as

$$\mathbb{E}(|X\rangle) = \frac{\cos(4z) + 1}{3}.\tag{15}$$

Similarly for other values, also we can obtain the simplified expression for the GME-AME measure and are expressed as follows: (1) For the vertex CNOT to DCNOT, for the values $(\pi/4,0,0)$ to $(\pi/4,\pi/4,0)$, the GME-AME measure reduces to a single parameter family as .

$$\mathbb{E}(|X\rangle) = \frac{2}{10} \left(\cos(4y) - \frac{10}{9} \right) \left(\sin^4 \left(\frac{y + \frac{\pi}{4}}{2} \right) + \cos^4 \left(\frac{y + \frac{\pi}{4}}{2} \right) - 1 \right). \tag{16}$$

(2) For the vertex CNOT to SWAP, $(\pi/4,0,0)$ to $(\pi/4,\pi/4,\pi/4)$, the GME-AME measure is

$$\mathbb{E}(|X\rangle) = \left(1.7\sin^2\left(\frac{\pi}{4} + y\right)\cos^2(2z)\cos^2\left(\frac{\pi}{4} + y\right) - \frac{4}{3}\right) \times \left(\sin^2(2z) + \sin^2\left(\frac{\pi}{4} + y\right) + \cos^2\left(\frac{\pi}{4} + y\right) - 1\right). \tag{17}$$

(3) For the vertex LOCAL to DCNOT, (0,0,0) to $(\pi/4,\pi/4,0)$

$$\mathbb{E}(|X\rangle) = \left(4.0\sin^2(x)\sin^2(y)\cos^2(x)\cos^2(y) - 0.75\right)$$

$$\left(0.22(1-\cos(2x))^2(1-\cos(2y))^2 + 0.22(\cos(2x)+1)^2(\cos(2y)+1)^2 - 0.88\cos(2x-2y) - 0.88\cos(2x+2y) - 1.78\right).$$
(18)

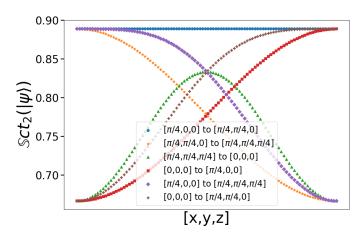


Figure 4. The Scott measure $Sct_2(|X\rangle)$ for qubits, with the plot generated from 100 data points obtained by varying the parameters [x, y, z].

The Scott measure, Eq. (2) and the Polygon measure in Eq. (6)is calculated for the parameterized state $|X\rangle$. The detailed plots for all the values of [x,y,z] from the Weyl chamber is plotted for Scott measure in Fig.(4) and the Polygon measure in the Fig. (3). The Scott measure can be evaluated analytically, and given as

$$Sct_2(|X\rangle) = \frac{4}{3} - \frac{1}{18}f(x, y, z)$$
 (19)

where

$$f(x,y,z) = 2 + 4\cos^{4}(x - y) + (-1 + \sin(2x)\sin(2y))^{2} + (1 + \sin(2x)\sin(2y))^{2} + (\sin^{2}(x - y) + \sin^{2}(x + y))^{2} + 4\cos^{2}(2z)(\cos^{2}(x - y)\cos^{2}(x + y) + \sin^{4}(x + y)) - (-2 + \cos(4x) + \cos(4y))\sin^{2}(2z)$$
(20)

which shows similar behavior to that of the GME-AME

measure but differing the fact that it is unable to detect the non-GME states. The Polygon measure differs predominently with the GME-AME measure. It detects the

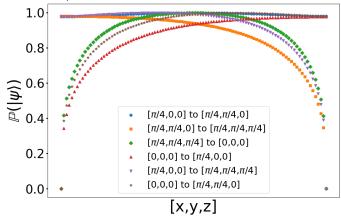


Figure 5. The Polygon measure $\mathbb{P}(|\psi\rangle)$ of $|X\rangle$. The state shows $\mathbb{P}=0$ for the specific parameter sets [x,y,z]=[0,0,0] and $[\pi/4,\pi/4,\pi/4]$, while exhibiting non-zero values for all other parameter combinations.

GME state successfully but fails to detect the AME, as it will reach maximum value even for non-AME states.

For three qubit states, GHZ and W states are two LOCC inequivalent classes [10]. For four qubit states there are continous family of LOCC inequivalent classes divided into nine distinct classes [65]. The GME-AME values for the all these states are calculated and is presented in the Appendix. (A).

V. FOUR PARTY PERMUTATION STATES

No.	$\mathbb{E}(P\rangle)$	States	No.	$\mathbb{E}(P\rangle)$	States	No.	$\mathbb{E}(P\rangle)$	States	No.	$\mathbb{E}(P\rangle)$	States	No.	$\mathbb{E}(P\rangle)$	States	No.	$\mathbb{E}(P\rangle)$	States
1	0.0000	72	7	0.6667	13608	13	0.7222	2592	19	0.6420	5184	24	0.7176	10368	29	0.7654	64800
2	0.4444	1296	8	0.6713	10368	14	0.7346	5184	20	0.7894	10368	25	0.8148	15552	30	0.8056	5184
3	0.5000	864	9	0.6821	10368	15	0.7407	10368	21	0.6667	13608	26	0.7222	2592	31	0.7901	34344
4	0.5093	1296	10	0.6914	12960	16	0.7415	25920	22	0.8133	25920	27	0.8395	20736	32	0.8920	2592
5	0.6019	1296	11	0.6944	3456	17	0.7500	288	23	0.8889	1296	28	0.8403	1728	33	1.0000	72
6	0.6296	5184	12	0.7160	23328	18	0.7608	36288									

Table I. The GME-AME value $\mathbb{E}(|P\rangle)$ for the permutation qutrit states. It shows 33 classes of permutation states are there out of 9!=362880 states

In quantum information theory, permutation matrices play a fundamental role in describing the rearrangement of subsystems in composite quantum systems. These matrices are used to model the swapping of qubits or higher-dimensional quantum states (qudits) and are integral in the study of entanglement, error correction, and quantum algorithms. A permutation matrix is a square unitary matrix that has exactly one entry of 1 in each row and each column, with all other entries being 0.

Let *P* represent the permutation matrix of size $d^2 \times d^2$ defined on the bipartite Hilbert space $\mathcal{H}_d \otimes \mathcal{H}_d$,

$$P\left|ij\right\rangle = \left|m_{ij}n_{ij}\right\rangle,\tag{21}$$

such that the operator and corresponding permutation state is defined as

$$P = \sum_{ij} |m_{ij}n_{ij}\rangle\langle ij|$$

$$|P\rangle = \sum_{ij} |m_{ij}n_{ij}\rangle|ij\rangle$$
(22)

and the corresponding four party state is represented as $|P\rangle$. In this section, we study the entanglement structure of these states for local dimension d=2 and d=3.

For any dimension d there are d^2 ! number of permutation operators can be defined. For d = 2, there are 24 permutation operators and corresponding 24 perumtation states $|P\rangle$. We have calculated the GME-AME measure, Scott measure and Polygon measure and plotted in the Fig. (6). It can be seen that there are two classes states having minimum and maximum, which is evident from all the three measures. There are 8 permutation states that are non-GME and remaining 16 states are GME states maximizing the respective measures. For GME-AME measure, and for the Polygon measure, all 8 permutation operators reaches its minimum 0, and the remaining 16 permutation states reach the maximum value 0.3 for the GME-AME measure 0.7 for Scott measure and the value 0.96 for the Polygon measure.

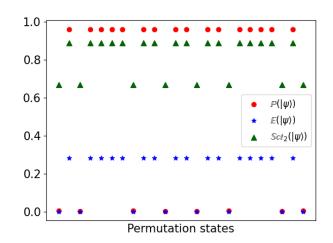


Figure 6. $\mathbb{E}(|P\rangle)$, $\mathrm{S}ct_2(|P\rangle)$ and $\mathbb{P}(|P\rangle)$ of qubit permutation state.

Interesting way to change the entanglement structure is *enphasing* the permutation states by introducing the arbitrary phase [59],

$$P = \sum_{ij} e^{i\theta_{ij}} |ij\rangle \langle l_{ij}k_{ij}|$$

$$|P\rangle = \sum_{ij} e^{i\theta_{ij}} |ij\rangle \langle l_{ij}k_{ij}|.$$
(23)

For d=2, such enphasing for $\theta_{ij}\in\{0,\pi\}$ is considered for a both the class of permutation operators and the variation of various measures is plotted. For the the permutation state having either 0 value (non-GME) or minimum value (in case of Scott measure), enphasing produces $\mathbb{E}(|\psi\rangle)$ values that range from 0.0 to 0.3 Fig : (7 case of GME-AME measure, 0.2 to 0.96 value in case of polygon measure Fig : 14, 0.66 to 0.88 in case of Scott measure Fig : 13. In contrast, for the GME states , enphasing yields a constant for all three measures .

For d = 3, there are 9! = 362880 permutation operators and the GME-AME measure and the Scott measure is calculated for these states. The GME-AME measure is plotted in Fig (8), and the Scott measure is in Fig. (9).

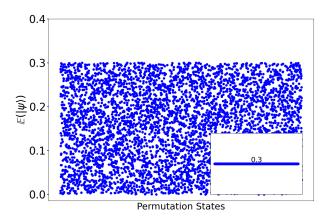


Figure 7. The GME-AME measure $\mathbb{E}(|\psi\rangle)$ of enphased permutation state by enphasing the permutation having $\mathbb{E}|\psi\rangle=0$ and the inset one is the enphased with the permutation having $\mathbb{E}|\psi\rangle=0.3$.

It can be seen that there are totally 72 states are non-GME and also there are 72 states that are AME states. The GME-AME measure is more robust in clasifying the various classes as there are totally 33 classes of permutation states according to GME-AME where as totally 16 classes are detected through the Scott measure. The exact values and the number of permutation states in these classes are listed in the table (II) for GME-AME measure and in table (I) for Scott measure.

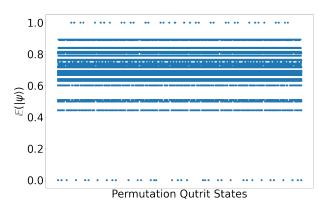


Figure 8. The GME-AME $\mathbb{E}(|P\rangle)$ for the permutation of a qutrit state. Among the 9! = 362,880 possible states, 33 distinct $\mathbb{E}(|P\rangle)$ values are observed.

VI. CONCLUSION AND DISCUSSIONS

In this study, we introduced the GME-AME measure to detect both genuine multipartite entanglement and absolutely maximally entangled states. The measure has a defined range with a lower bound of o for non-GME states and an upper bound of 1 for AME states. The GME-AME measure is applied to study four par-

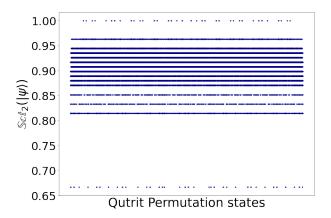


Figure 9. The Scott measure $\mathbf{Sct}_2(|P\rangle)$ for the permutation of a qutrit state. Among the 9! = 362,880 possible states, 16 distinct $\mathbb{E}(|P\rangle)$ values are observed.

No.	$\mathbb{S}ct_2((\psi\rangle)$	States	No	$\mathbb{S}ct_2((\psi\rangle)$	States
1	0.6667	72	9	0.8889	27432
2	0.8148	1170	10	0.8981	36288
3	0.8333	864	11	0.9167	101376
4	0.8148	1422	12	0.9352	46656
5	0.8796	20736	13	0.8519	1296
6	0.8704	10368	14	0.9074	44064
7	0.8889	27432	15	0.9259	44712
8	0.9630	3888	16	1.0000	72

Table II. Table of $Sct_2(|P\rangle)$ values of permutation qutrit states ,There are 16 classes of $\mathbb E$ permutation states are there out of 9!=362880 states

tite states using operator to state mapping for various classes of four party qubit states and permutation states for the qubits and qutrits. We have compared our results with other independent measures of GME and AME and found that the GME-AME measure proposed in this work is robust in classifying the multipartite entangled states.

The main interesting extensions of the work relate to applying it for a higher number of parties and applying the GME-AME measure in the quantum information theoretic tasks. In the case of many-body systems, it is interesting to see the entanglement growth by considering the entire many-body system as a four-partite system and see the nature of entanglement growth. It is also interesting to see the efficiency of calculating this in the quantum computer for a higher number of parties. The concentratable entanglement is used to classify the multipartite entangled states in a hierarchy [66]. The non-zero value of concentratable entanglement does not guarantee GME; hence, constructing the hierarchy in terms of GME-AME states would give further insights into the multipartite entanglement structure.

VII. ACKNOWLEDGEMENTS

SA acknowledges the start-up research grant from SERB, Department of Science and Technology, Govt. of India (SRG/2022/000467). Authors thank Ranjan Modak, Nripendra Majumdar and Songbo Xie for helpful discussions.

- [1] Albert Einstein, Boris Podolsky, and Nathan Rosen, "Can quantum-mechanical description of physical reality be considered complete?" Physical review 47, 777 (1935).
- [2] Ryszard Horodecki, Paweł Horodecki, Michał Horodecki, and Karol Horodecki, "Quantum entanglement," Reviews of Modern Physics 81, 865 (2009).
- [3] Charles H Bennett, Gilles Brassard, Claude Crépeau, Richard Jozsa, Asher Peres, and William K Wootters, "Teleporting an unknown quantum state via dual classical and einstein-podolsky-rosen channels," Physical review letters 70, 1895 (1993).
- [4] Charles H. Bennett and Gilles Brassard, "Quantum cryptography: Public key distribution and coin tossing," in *Proceedings of IEEE International Conference on Computers, Systems and Signal Processing* (IEEE, Bangalore, India, 1984) pp. 175–179.
- [5] Pasquale Calabrese and John Cardy, "Entanglement entropy and quantum field theory," Journal of Statistical Mechanics: Theory and Experiment 2004, Po6002 (2004).
- [6] Mark Van Raamsdonk, "Lectures on gravity and entanglement," in New Frontiers in Fields and Strings: TASI 2015 Proceedings of the 2015 Theoretical Advanced Study Institute in Elementary Particle Physics (World Scientific, 2017) pp. 297–351.
- [7] Luigi Amico, Rosario Fazio, Andreas Osterloh, and Vlatko Vedral, "Entanglement in many-body systems," Rev. Mod. Phys. 80, 517–576 (2008).
- [8] Robert Raussendorf and Hans J Briegel, "A one-way quantum computer," Physical review letters **86**, 5188 (2001).
- [9] Otfried Gühne and Géza Tóth, "Entanglement detection," Physics Reports 474, 1–75 (2009).
- [10] Wolfgang Dür, Guifré Vidal, and J Ignacio Cirac, "Three qubits can be entangled in two inequivalent ways," Physical Review A 62, 062314 (2000).
- [11] Eric Chitambar and Gilad Gour, "Everything you always wanted to know about locc (but were afraid to ask)," Communications in Mathematical Physics 326, 1–48 (2014).
- [12] Christopher Eltschka and Jens Siewert, "Multipartite entanglement measures," Journal of Physics A: Mathematical and Theoretical 47, 424005 (2014).
- [13] M. Murao, D. Jonathan, M. B. Plenio, and V. Vedral, "Multiparticle entanglement purification for two-colorable graph states," Phys. Rev. A 62, 062314 (2000).
- [14] Michiel Seevinck, "Multipartite bell-type inequalities for entanglement detection," Quantum 1, 9 (2017).
- [15] Nicolas Brunner, Daniel Cavalcanti, Stefano Pironio, Valerio Scarani, and Stephanie Wehner, "Bell nonlocality,"

- Reviews of Modern Physics 86, 419–478 (2014).
- [16] Daniel Collins, Nicolas Gisin, Sandu Popescu, David Roberts, and Valerio Scarani, "Bell-type inequalities to detect true n-body nonseparability," Physical review letters 88, 170405 (2002).
- [17] Jos Uffink, "Quadratic bell inequalities as tests for multipartite entanglement," Physical Review Letters 88, 230406 (2002).
- [18] Michael Seevinck and Jos Uffink, "Partial separability and entanglement criteria for multiqubit quantum states," Physical Review A—Atomic, Molecular, and Optical Physics 78, 032101 (2008).
- [19] Wolfram Helwig, Wei Cui, José Ignacio Latorre, Arnau Riera, and Hoi-Kwong Lo, "Absolute maximal entanglement and quantum secret sharing," Physical Review A 86, 052335 (2012).
- [20] Lieven Clarisse, Sibasish Ghosh, Simone Severini, and Anthony Sudbery, "Entangling power of permutations," Physical Review A—Atomic, Molecular, and Optical Physics 72, 012314 (2005).
- [21] Dardo Goyeneche, Zahra Raissi, Sara Di Martino, and Karol Życzkowski, "Entanglement and quantum combinatorial designs," Physical Review A 97, 062326 (2018).
- [22] Dardo Goyeneche, Daniel Alsina, José I Latorre, Arnau Riera, and Karol Życzkowski, "Absolutely maximally entangled states, combinatorial designs, and multiunitary matrices," Physical Review A 92, 032316 (2015).
- [23] Suhail Ahmad Rather, N Ramadas, Vijay Kodiyalam, and Arul Lakshminarayan, "Absolutely maximally entangled state equivalence and the construction of infinite quantum solutions to the problem of 36 officers of euler," Physical Review A 108, 032412 (2023).
- [24] F Huber and N Wyderka, "Table of ame states," disponible en línea en http://www. tp. nt. uni-siegen. de/+ fhuber/ame. html (2020).
- [25] A. Higuchi and A. Sudbery, "How entangled can two couples get?" Physics Letters A 273, 213 217 (2000).
- [26] Zhi-Hao Ma, Zhi-Hua Chen, Jing-Ling Chen, Christoph Spengler, Andreas Gabriel, and Marcus Huber, "Measure of genuine multipartite entanglement with computable lower bounds," Physical Review A—Atomic, Molecular, and Optical Physics 83, 062325 (2011).
- [27] Abner Shimony, "Degree of entanglement a," Annals of the New York Academy of Sciences 755, 675–679 (1995).
- [28] Howard Barnum and Noah Linden, "Monotones and invariants for multi-particle quantum states," Journal of Physics A: Mathematical and General 34, 6787 (2001).
- [29] Tzu-Chieh Wei and Paul M. Goldbart, "Geometric measure of entanglement and applications to bipartite and

- multipartite quantum states," Physical Review A **68**, 042307 (2003).
- [30] Songbo Xie and Joseph H Eberly, "Triangle measure of tripartite entanglement," Physical Review Letters 127, 040403 (2021).
- [31] Songbo Xie, Xuan Zhang, and Jiaqi Li, "A triangle measure for three-qubit systems," Physical Review A 105, 052427 (2022).
- [32] Songbo Xie, Daniel Younis, Yuhan Mei, and Joseph H Eberly, "Multipartite entanglement: A journey through geometry," Entropy 26, 217 (2024).
- [33] Ansh Mishra, Soumik Mahanti, Abhinash Kumar Roy, and Prasanta K Panigrahi, "Geometric genuine multipartite entanglement for four-qubit systems," Physics Open **20**, 100230 (2024).
- [34] O. Gühne and M. Seevinck, "Separability criteria for genuine multiparticle entanglement," New Journal of Physics 12, 053002 (2010).
- [35] Sam A Hill and William K Wootters, "Entanglement of a pair of quantum bits," Physical review letters **78**, 5022 (1997).
- [36] Samgeeth Puliyil, Manik Banik, and Mir Alimuddin, "Thermodynamic signatures of genuinely multipartite entanglement," Physical Review Letters 129, 070601 (2022).
- [37] Valerie Coffman, Joydip Kundu, and William K Wootters, "Distributed entanglement," Physical Review A 61, 052306 (2000).
- [38] Alexander Wong and Nelson Christensen, "Potential multiparticle entanglement measure," Physical Review A 63, 044301 (2001).
- [39] David A Meyer and Nolan R Wallach, "Global entanglement in multiparticle systems," Journal of Mathematical Physics 43, 4273–4278 (2002).
- [40] Michael Walter, Brent Doran, David Gross, and Matthias Christandl, "Entanglement polytopes: multiparticle entanglement from single-particle information," Science 340, 1205–1208 (2013).
- [41] André RR Carvalho, Florian Mintert, and Andreas Buchleitner, "Decoherence and multipartite entanglement," Physical review letters **93**, 230501 (2004).
- [42] Jacob L Beckey, N Gigena, Patrick J Coles, and M Cerezo, "Computable and operationally meaningful multipartite entanglement measures," Physical Review Letters 127, 140501 (2021).
- [43] Vittorio Giovannetti, Seth Lloyd, and Lorenzo Maccone, "Advances in quantum metrology," Nature photonics 5, 222–229 (2011).
- [44] Massimiliano Proietti, Joseph Ho, Federico Grasselli, Peter Barrow, Mehul Malik, and Alessandro Fedrizzi, "Experimental quantum conference key agreement," Science Advances 7, eabeo395 (2021).
- [45] P. Hyllus and et al., "Multiparticle interference and quantum metrology," Physical Review A 85, 043630 (2012).
- [46] Y. Liu and et al., "Genuine multipartite entanglement distribution in quantum networks," Quantum Science and Technology **5** (2020), 10.1088/2058-9565/ab5e2f.
- [47] Zahra Raissi, Christian Gogolin, Arnau Riera, and Antonio Acín, "Optimal quantum error correcting codes from absolutely maximally entangled states," Journal of Physics A: Mathematical and Theoretical 51, 075301

- (2018).
- [48] Daniel Alsina and Mohsen Razavi, "Absolutely maximally entangled states, quantum-maximum-distance-separable codes, and quantum repeaters," Physical Review A 103, 022402 (2021).
- [49] Fernando Pastawski, Beni Yoshida, Daniel Harlow, and John Preskill, "Holographic quantum error-correcting codes: Toy models for the bulk/boundary correspondence," Journal of High Energy Physics 2015, 1–55 (2015).
- [50] Andrew J Scott, "Multipartite entanglement, quantumerror-correcting codes, and entangling power of quantum evolutions," Physical Review A—Atomic, Molecular, and Optical Physics **69**, 052330 (2004).
- [51] Karol Życzkowski and Ingemar Bengtsson, "On duality between quantum maps and quantum states," Open Systems & Information Dynamics 11, 3–42 (2004).
- [52] Ingemar Bengtsson and Karol Życzkowski, *Geometry of quantum states: an introduction to quantum entanglement* (Cambridge University Press, 2007).
- [53] Kai Chen and Ling-An Wu, "A matrix realignment method for recognizing entanglement," arXiv preprint quant-ph/0205017 (2002).
- [54] Oliver Rudolph, "Some properties of the computable cross-norm criterion for separability," Physical Review A **67**, 032312 (2003).
- [55] Clinton J Oxenrider and Richard D Hill, "On the matrix reorderings γ and ψ ," Linear algebra and its applications **69**, 205–212 (1985).
- [56] ECG Sudarshan, PM Mathews, and Jayaseetha Rau, "Stochastic dynamics of quantum-mechanical systems," Physical Review 121, 920 (1961).
- [57] M Akila, D Waltner, B Gutkin, and T Guhr, "Particletime duality in the kicked Ising spin chain," Journal of Physics A: Mathematical and Theoretical **49**, 375101 (2016).
- [58] Bruno Bertini, Pavel Kos, and Tomaž Prosen, "Exact correlation functions for dual-unitary lattice models in 1+1 dimensions," Phys. Rev. Lett. **123**, 210601 (2019).
- [59] Suhail Ahmad Rather, S. Aravinda, and Arul Lakshminarayan, "Creating ensembles of dual unitary and maximally entangling quantum evolutions," Phys. Rev. Lett. **125**, 070501 (2020).
- [60] S. Aravinda, Suhail Ahmad Rather, and Arul Lakshminarayan, "From dual-unitary to quantum Bernoulli circuits: Role of the entangling power in constructing a quantum ergodic hierarchy," Phys. Rev. Research 3, 043034 (2021).
- [61] Suhail Ahmad Rather, S Aravinda, and Arul Lakshminarayan, "Construction and local equivalence of dual-unitary operators: from dynamical maps to quantum combinatorial designs," PRX Quantum 3, 040331 (2022).
- [62] Navin Khaneja, Roger Brockett, and Steffen J. Glaser, "Time optimal control in spin systems," Phys. Rev. A 63, 032308 (2001).
- [63] B. Kraus and J. I. Cirac, "Optimal creation of entanglement using a two-qubit gate," Phys. Rev. A 63, 062309 (2001).
- [64] Jun Zhang, Jiri Vala, Shankar Sastry, and K. Birgitta Whaley, "Geometric theory of nonlocal two-qubit operations," Phys. Rev. A 67, 042313 (2003).

- [65] Frank Verstraete, Jeroen Dehaene, Bart De Moor, and Henri Verschelde, "Four qubits can be entangled in nine different ways," Physical Review A 65, 052112 (2002).
- [66] Louis Schatzki, Guangkuo Liu, Marco Cerezo, and Eric Chitambar, "Hierarchy of multipartite correlations based on concentratable entanglement," Physical Review Research 6, 023019 (2024).

Appendix A: 9 different classes in 4 party qubit states

In the four-partite case, there are nine distinct classes of entanglement, where any qubit state of a four-partite system can be transformed into one of these classes via LOCC transformations [65]. A detailed investigation of these states reveals that the $|G_{abcd}\rangle$ class corresponds to the same class as the $|X\rangle$ state. Moreover, only the $|L_{0_3\oplus 1}0_{3\oplus 1}\rangle$ state has an GME-AME measure of zero. For the remaining classes, the GME-AME measure is non-zero, indicating that they are genuinely multipartite entangled (GME) states.The following 9 clsses are as:

$$\begin{split} |G_{abcd}\rangle &= \frac{a+d}{2}(|0000\rangle + |1111\rangle) + \frac{a-d}{2}(|0011\rangle + |1100\rangle) + \frac{b+c}{2}(|0101\rangle + |1010\rangle) + \frac{b-c}{2}(|0110\rangle + |1001\rangle) \\ |L_{abc_2}\rangle &= \frac{a+b}{2}(|0000\rangle + |1111\rangle) + \frac{a-b}{2}(|0011\rangle + |1100\rangle) + c(|0101\rangle + |1010\rangle) + |0110\rangle \\ |L_{a_2b_2}\rangle &= a(|0000\rangle + |1111\rangle) + b(|0101\rangle + |1010\rangle) + |0110\rangle + |0011\rangle \\ |L_{ab_3}\rangle &= a(|0000\rangle + |1111\rangle) + \frac{a+b}{2}(|0101\rangle + |1010\rangle) + \frac{a-b}{2}(|0110\rangle + |1001\rangle) + \frac{i}{\sqrt{2}}(|0001\rangle + |0010\rangle) + (|0111\rangle + |1011\rangle) \\ |L_{a_4}\rangle &= a(|0000\rangle + |0101\rangle + |1010\rangle + |1111\rangle) + (i|0001\rangle + |0110\rangle - i|1011\rangle) \\ |L_{a_2 \oplus 0_{3 \oplus 1}}\rangle &= a(|0000\rangle + |0101\rangle + |1000\rangle) + |1110\rangle \\ |L_{0_{5 \oplus 3}}\rangle &= (|0000\rangle + |0101\rangle + |1010\rangle) + |1110\rangle \\ |L_{0_{5 \oplus 3}}\rangle &= (|0000\rangle + |0101\rangle + |1101\rangle + |1110\rangle) \\ |L_{0_{5 \oplus 1}0_{3 \oplus 1}}\rangle &= (|0000\rangle + |0111\rangle) + |1110\rangle \\ |L_{0_{5 \oplus 1}0_{3 \oplus 1}}\rangle &= (|0000\rangle + |0111\rangle) \end{split}$$

The state $\left|L_{0_3\oplus 1^0_3\oplus 1}\right\rangle$ state has an GME-AME measure zero. For the remaining classes, the GME-AME measure is non-zero, indicating that they are GME states. The GME-AME $\mathbb E$ values for all classes are calculated and given below.For $\left|L_{abc_2}\right\rangle$ the GME-AME measure $\mathbb E$ value between 0.25 and 0.55 Fig. 10, $\left|L_{a_2b_2}\right\rangle$ ranges from 0.3 to 0.475 Fig. 11 and $\left|L_{a_2b_2}\right\rangle$ from 0.03 to 0.26, Fig. 12. The calculated values of $\mathbb E(\left|L_{a_4}\right\rangle) = 0.4$, $\mathbb E(\left|L_{a_20_3\oplus 1}\right\rangle) = 0.23$, $\mathbb E(\left|L_{0_5\oplus 3}\right\rangle) = 0.156$, $\mathbb E(\left|L_{0_7\oplus 1}\right\rangle) = 0.435$, $\mathbb E(\left|L_{0_3\oplus 1}_{0_{3\otimes 1}}\right\rangle) = 0$

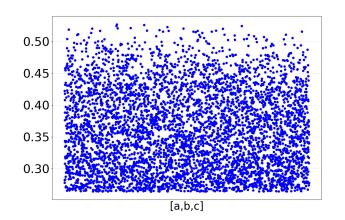


Figure 10. $\mathbb{E}(|L_{abc_2}\rangle)$ For different 1000 [a,b,c] values

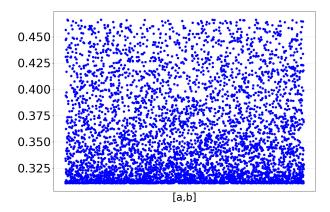


Figure 11. $\mathbb{E}(\left|L_{a_2b_2}\right\rangle)$ For different 1000 [a,b,c] values

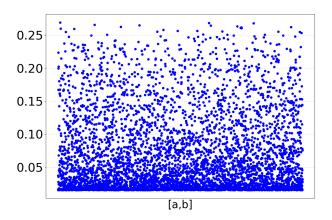


Figure 12. $\mathbb{E}(\left|L_{ab_3}\right\rangle)$ For different 1000 [a,b,c] values

Appendix B: Enphasing of Permutation states

In this Section, we provide the plots for the Scott measure and Polygon measure for the enphasing of qubit permutation states.

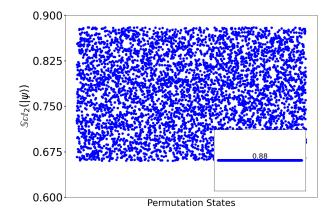


Figure 13. $Sct_2 |P\rangle$ enphasing qubit permutation state.

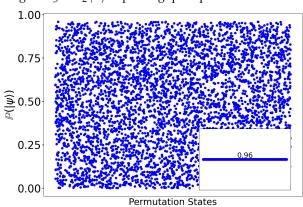


Figure 14. The polygon measure of $\mathbb{P}(|P\rangle)$ enphased qubit permutation states.